Nonreciprocal magnon-photon-phonon entanglement in cavity magnomechanics

Subhadeep Chakraborty [1] and Camelia Das [2]

[1] *Centre for Quantum Engineering, Research and Education, TCG CREST, Salt Lake, Kolkata 700091, India*

[2] *Department of Physics, Faculty of Science and Technology, ICFAI University Tripura, Agartala 799210, Tripura (W), India*

(Received 3 June 2023; accepted 13 November 2023; published 6 December 2023)

We propose a scheme to create nonreciprocal entanglement in a spinning cavity magnomechanical system. The setup comprises a whispering gallery mode resonator with two counterpropagating modes, simultaneously coupled to yttrium iron garnet. By spinning the resonator, the counterpropagating modes undergo an opposite Fizeau drag caused by the optical Sagnac effect. We show that in a spinning resonator, the cavity-magnon-phonon modes get entangled along a chosen direction while remaining fully uncorrelated in the other. The degree of nonreciprocity is determined by the drive detuning and the spinning velocity of the resonator. Our work provides a different route to achieve chiral control of quantum entanglement involving magnon-photon-phonon modes.

DOI: 10.1103/PhysRevA.108.063704

I. INTRODUCTION

Nonreciprocal physics has become an actively pursued field of research in recent times, having a wide range of applications in invisible sensing or cloaking and noise-free information processing [1]. Of particular interest here is electromagnetic nonreciprocity where magneto-optical materials are commonly used to break the time-reversal symmetry. While these magnet-based devices are difficult to integrate and miniaturize, there has been an ongoing search for chip-compatible nonmagnetic optical isolators and circulators. Nonlinear optics [2,3], optomechanics [4–7], non-Hermitian optics [8,9], and atomic gases [10–13] are a few of the optical devices where nonreciprocity has been achieved. Further achievements include the demonstration of acoustic and electronic one-way devices [14–18]. However, most of the studies reported so far are primarily driven towards the classical regime, focusing on the transmission-rate nonreciprocity. It is only recently that nonreciprocal quantum devices have been explored. Along this line, based on the Fizeau light-dragging effect [19], very recently, proposals for nonreciprocal photon blockade [20,21] and backscattering immune optomechanical entanglement [22] have received considerable attention.

Cavity magnonics [23,24] is, on the other hand, a relatively young field that seeks to explore the interaction between a magnon, the elementary excitation of magnetization, and a cavity photon. In its simplest form, such a system comprises an electromagnetic cavity with a magnetic material placed inside it. The magnetic material of choice here is yttrium iron garnet (YIG), a ferrimagnetic insulator with high spin density and a low damping rate. With strongly coupled magnon-photon modes [25], cavity magnonics shows potential application prospects in quantum information processing, acting as either a quantum transducer [26–30] or memory [31]. In addition, because of the magnetostrictive force, magnons can also couple to vibrational phonons [32]. Combining these concepts, a magnon coupled to both an electromagnetic cavity and a mechanical resonator, have given rise to a whole new field of cavity magnomechanics. Some of the recent studies subjected to magnomechanical systems are magnomechanically induced transparency [32–34], phonon lasers [32,35], magnon-induced dynamical backaction [36], ground-state cooling of magnomechanical resonators [37], magnomechanical storage and retrieval of quantum states [38], magnon chaos [39], and so on.

Another stimulating direction is to observe the nonclassical states in magnonics [40]. Being typically of a size of 100 μm, YIG provides an alternative route to probe the macroscopic quantum effects, entanglement, and squeezing, for instance. To date, cavity optomechanics [41] has been the most successful candidate in realizing such nonclassical states in micro- and nanomechanical oscillators. Apart from a plethora of theoretical studies [42], there are also, in fact, experimental demonstrations of entangling massive mechanical oscillators [43–45]. However, as compared to the opto- or electromechanical systems, magnonics appear to be the better tunable ones, allowing an external magnetic field to control the magnon frequency. The proposal for creating magnon-photon-phonon entanglement was first studied in Ref. [46]. This has inspired a series of theoretical works on squeezing the magnon mode [47] and entangling two magnon modes [48–52], two cavity modes [53], and also two phonon modes [54], in a cavity-magnon-phonon setup.

In parallel, cavity magnonics has been studied in the context of nonreciprocal physics. Very recently, by harnessing the cooperative effect of coherent and dissipative magnon-photon coupling, nonreciprocal microwave transmission has been realized in an open cavity-magnon system [55]. A theoretical framework to achieve microwave circulation has also been studied in a multimode cavity-magnon system [56]. Moreover, exploiting the same Fizeau light-dragging effect, there are proposals of nonreciprocal magnon [57] and phonon [58] lasers. Also, very recently, in a similar setup of a spinning magnomechanical resonator, the nonreciprocal transmission rate and magnon-phonon entanglement have been studied [59,60]. These motivate us to study the nonreciprocal formation of quantum entanglement in a cavity magnomechanical

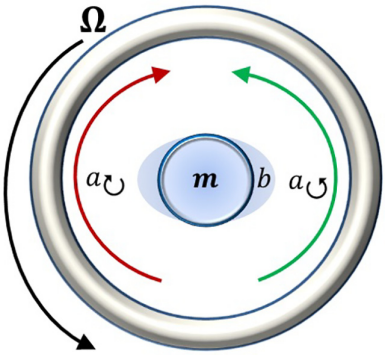

FIG. 1. Schematic of the proposed model. A YIG sphere is placed inside a spinning WGM resonator. The WGM resonator supports two counterpropagating modes, while the YIG hosts both a magnon mode and a phonon mode.

setup. In particular, we are primarily focused here to observe such an effect in a somewhat more complicated tripartite entanglement including the magnon-photon-phonon modes. We note that our scheme works well for creating nonreciprocal bipartite entanglements involving both the magnon-photon and magnon-phonon modes. This work could be of particular relevance to several applications in quantum information processing and quantum computing [61,62].

II. SYSTEM AND ITS STEADY STATE

As schematically shown in Fig. 1, we consider a cavity magnomechanical system that comprises a YIG sphere placed in the center (where the magnetic field is maximum) of a spinning whispering gallery mode (WGM) resonator. The WGM resonator supports two counterpropagating modes that experience a Fizeau shift when spinning the resonator. By fixing the counterclockwise (CCW) spinning direction, the circulating clockwise (CW) and counterclockwise (CCW) mode frequencies respectively read as $\omega_{\circlearrowleft} = \omega_c + \Delta_F$ and $\omega_{\circlearrowright} = \omega_c - \Delta_F$, where ω_c is the optical resonance frequency of the nonspinning resonator and

$$\Delta_F = \pm\Omega\frac{nr\omega_c}{c}\left(1 - \frac{1}{n^2} - \frac{\lambda}{n}\frac{dn}{d\lambda}\right) \tag{1}$$

is the amount of the Fizeau shift [19,63]. The parameters Ω, n, and r respectively characterize the spinning velocity, refractive index, and radius of the resonator, and c (λ) is the light velocity (wavelength) in vacuum. The dissipation term $dn/d\lambda$ incorporates the relativistic correction to the Fizeau light-dragging effect, which is relatively small, and thus neglected. The YIG sphere embodies, simultaneously, a magnon mode of frequency ω_m and a phonon mode of frequency ω_b. The Hamiltonian of such a system can be written as

$$\begin{aligned} H = &\sum_{j=\circlearrowleft,\circlearrowright}[\omega_j a_j^\dagger a_j + g_{ma}(m^\dagger a_j + a_j^\dagger m)] + \omega_m m^\dagger m \\ &+ \frac{\omega_b}{2}(q^2 + p^2) + g_{mb} m^\dagger m q + H_{\rm drive}, \end{aligned} \tag{2}$$

where a ($a^\dagger$) and m ($m^\dagger$) ($[O, O^\dagger] = 1, O = a, m$) are the annihilation (creation) operators of the cavity and the magnon modes, respectively, and q and p ($[q, p] = i$) are the dimensionless position and momentum operators of the phonon mode. g_{ma} and g_{mb} are respectively the coupling strengths between the magnon and photon and the (single) magnon and phonon modes. A typical parameter regime is where the magnon-photon interaction lies in the strong-coupling regime, while the magnon-phonon interaction is very weak. Nevertheless, this coupling (g_{mb}) can further be enhanced by reducing the diameter (D) of the YIG sphere as $g_{mb} \propto 1/D^2$ [32]. Finally, we consider the drive Hamiltonian $H_{\rm drive} = i\epsilon(e^{-i\omega_d t}a_\eta^\dagger - e^{i\omega_d t}a_\eta)$, where $\eta \in (\circlearrowleft, \circlearrowright)$ fixes the driving direction and ϵ gives the driving amplitude. In a frame rotating at the drive frequency ω_d, the quantum Langevin equations of the system are given by

$$\begin{aligned} \dot{a}_{\circlearrowleft} &= -(i\Delta_{\circlearrowleft} + \kappa_a)a_{\circlearrowleft} - ig_{ma}m + \epsilon\delta_{\circlearrowleft,\eta} + \sqrt{2\kappa_a}a_{\circlearrowleft}^{\rm in}, \\ \dot{a}_{\circlearrowright} &= -(i\Delta_{\circlearrowright} + \kappa_a)a_{\circlearrowright} - ig_{ma}m + \epsilon\delta_{\circlearrowright,\eta} + \sqrt{2\kappa_a}a_{\circlearrowright}^{\rm in}, \\ \dot{m} &= -(i\Delta_m + \kappa_m)m - ig_{ma}(a_{\circlearrowleft} + a_{\circlearrowright}) - ig_{mb}mq \\ &\quad + \sqrt{2\kappa_m}m^{in}, \\ \dot{q} &= \omega_b p, \quad \dot{p} = -\omega_b q - \gamma_b p - g_{mb}m^\dagger m + \xi, \end{aligned} \tag{3}$$

where $\Delta_{\circlearrowleft,\circlearrowright} = \omega_{\circlearrowleft,\circlearrowright} - \omega_d$ ($\Delta_0 = \omega_c - \omega_d$) and $\Delta_m = \omega_m - \omega_d$ respectively denote the cavity and the magnon detuning. The decay rates of the cavity, magnon, and phonon modes are respectively κ_a, κ_m, and γ_b, while their associated input noise operators are $a_{\circlearrowleft,\circlearrowright}^{\rm in}$, $m^{\rm in}$, and ξ. These noises are zero-mean quantum Gaussian noises that obey the following correlation relations [64], $\langle a_j^{\rm in}(t)a^{{\rm in},\dagger}(t')\rangle = [N_j(\omega_c) + 1]\delta(t - t')$, $\langle a^{{\rm in},\dagger}(t)a^{\rm in}(t')\rangle = N_j(\omega_a)\delta(t - t')(j = \circlearrowleft, \circlearrowright)$, $\langle m_j^{\rm in}(t)m^{{\rm in},\dagger}(t')\rangle = [N_m(\omega_m) + 1]\delta(t - t')$, $\langle m^{{\rm in},\dagger}(t)m^{\rm in}(t')\rangle = N_m(\omega_m)\delta(t - t')$, and $\langle\xi(t)\xi(t') + \xi(t')\xi(t)\rangle/2 \simeq \gamma_b[2N_b(\omega_b) + 1]\delta(t - t')$, where $N_j = [\exp(\frac{\hbar\omega_j}{K_B T}) - 1]^{-1}$ is the mean equilibrium thermal occupation number at temperature T (and K_B is the Boltzmann constant and $j = a_{\circlearrowleft}, a_{\circlearrowright}, m, b$).

Driven by a strong external field, the cavity field amplitudes assume a large steady-state value $|\langle a_j\rangle| \gg 1$ ($j = \circlearrowleft, \circlearrowright$). In the presence of strong magnon-photon coupling this further enables us to rewrite each of these operators ($\mathcal{O} = a_{\circlearrowleft}, a_{\circlearrowright}, m, q, p$) as $\mathcal{O} = \langle\mathcal{O}\rangle + \delta\mathcal{O}$, where $\langle\mathcal{O}\rangle$ denotes the classical steady-state amplitudes and $\delta\mathcal{O}$ are the fluctuation operators. The steady-state amplitudes could be easily obtained as $\langle a_j\rangle = -(ig_{ma}\langle m\rangle - \epsilon\delta_{j,\eta})/(i\Delta_j + \kappa_a)$ [$\delta_{j,\eta} = 1(0)$ for $j = \eta(j \neq \eta)$ where $j \in [\circlearrowleft, \circlearrowright]$],

$$\langle m\rangle = -\frac{ig_{ma}\epsilon[\delta_{\circlearrowleft,\eta}(i\Delta_{\circlearrowleft} + \kappa_a) + \delta_{\circlearrowright,\eta}(i\Delta_{\circlearrowright} + \kappa_a)]}{(i\tilde{\Delta}_m + \kappa_m)(i\Delta_{\circlearrowleft} + \kappa_a)(i\Delta_{\circlearrowright} + \kappa_a) + g_{ma}^2(i\Delta_{\circlearrowleft} + i\Delta_{\circlearrowright} + 2\kappa_a)}, \tag{4}$$

$\langle q\rangle = -(g_{mb}/\omega_b)|\langle m\rangle|^2$, and $\langle p\rangle = 0$, where $\tilde{\Delta}_m = \Delta_m + g_{mb}\langle q\rangle$ includes the magnomechanical shift in the magnon detuning. As for the dynamics of the quantum fluctuations, we switch to the continuous-variable (CV) description and define the quadrature operators as $\delta x_j = (\delta a_j + \delta a_j^\dagger)/\sqrt{2}$, $\delta y_j = i(\delta a_j^\dagger - \delta a_j)/\sqrt{2}$ $(j = \circlearrowleft, \circlearrowright)$, $\delta X = (\delta m + \delta m^\dagger)/\sqrt{2}$, and $\delta Y = i(\delta m^\dagger - \delta m)/\sqrt{2}$, and similarly for the input noise operators. Neglecting all the second-order fluctuation terms, the linearized dynamics can be simply cast in the following matrix form,

$$\dot{u}(t) = Au(t) + n(t), \tag{5}$$

where $u(t) = [\delta x_\circlearrowleft(t), \delta y_\circlearrowleft(t), \delta x_\circlearrowright(t), \delta y_\circlearrowright(t), \delta X(t), \delta Y(t), \delta q(t), \delta p(t)]^T$ is the vector of quadrature fluctuation operators and $n(t) = [\sqrt{2\kappa_a}x^{\rm in}_\circlearrowleft(t), \sqrt{2\kappa_a}y^{\rm in}_\circlearrowleft(t), \sqrt{2\kappa_a}x^{\rm in}_\circlearrowright(t), \sqrt{2\kappa_a}y^{\rm in}_\circlearrowright(t), \sqrt{2\kappa_m}X^{\rm in}(t), \sqrt{2\kappa_m}Y^{\rm in}(t), 0, \xi(t)]^T$ is the vector of input noises. The drift matrix A is given by

$$\begin{pmatrix}
-\kappa_a & \Delta_\circlearrowleft & 0 & 0 & 0 & g_{ma} & 0 & 0\\
-\Delta_\circlearrowleft & -\kappa_a & 0 & 0 & -g_{ma} & 0 & 0 & 0\\
0 & 0 & -\kappa_a & \Delta_\circlearrowright & 0 & g_{ma} & 0 & 0\\
0 & 0 & -\Delta_\circlearrowright & -\kappa_a & -g_{ma} & 0 & 0 & 0\\
0 & g_{ma} & 0 & g_{ma} & -\kappa_m & \tilde{\Delta}_m & 0 & 0\\
-g_{ma} & 0 & -g_{ma} & 0 & -\tilde{\Delta}_m & -\kappa_m & -G_{mb} & 0\\
0 & 0 & 0 & 0 & 0 & 0 & 0 & \omega_b\\
0 & 0 & 0 & 0 & -G_{mb} & 0 & -\omega_b & -\gamma_b
\end{pmatrix}, \tag{6}$$

where $G_{mb} = \sqrt{2}g_{mb}\langle m\rangle$ is the effective magnon-phonon coupling strength. A formal solution of Eq. (5) reads as $u(t) = M(t)u(0) + \int_0^t dsM(s)n(t-s)$, where $M(t) = \exp(At)$. The system is said to be stable only for a set of all negative-real eigenvalues of A.

Due to the above linearized dynamics and zero-mean Gaussian nature of the quantum noises, the steady state is a quadripartite Gaussian state which is fully characterized by a 8×8 covariance matrix (CM) $V_{ij} = [\langle u_i(t)u_j(t') + u_j(t')u_i(t)\rangle]/2$. It is straightforward to show that the steady-state CM satisfies the following Lyapunov equation [65],

$$AV(\infty) + V(\infty)A^T = -D, \tag{7}$$

where $D = \text{diag}\,[\kappa_a(2N_\circlearrowleft + 1), \kappa_a(2N_\circlearrowright + 1), \kappa_a(2N_\circlearrowright + 1), \kappa_a(2N_\circlearrowleft + 1), \kappa_m(2N_m + 1), \kappa_m(2N_m + 1), 0, \gamma_b(2N_b + 1)]$ is the diffusion matrix, defined through $\langle n_i(t)n_j(t') + n_j(t')n_i(t)\rangle/2 = D_{ij}\delta(t-t')$.

III. ENTANGLEMENT MEASURES

To study the formation of bipartite and tripartite entanglement in our system, we respectively consider the logarithmic negativity E_N [66,67] and the *minimum* residual contangle $\mathcal{R}^{\rm min}$ [68] as the measures, where the contangle is the CV analog of discrete-variable tripartite entanglement [69]. The definition of CV logarithmic negativity reads as

$$E_N = \max[0, -\ln 2\tilde{\nu}_-], \tag{8}$$

where $\tilde{\nu}_- = \min|i\Omega_2\tilde{V}_4|$ (with the symplectic matrix $\Omega_2 = \oplus_{j=1}^2 i\sigma_y$ and $\sigma_y =$ y-Pauli matrix) is the minimum symplectic eigenvalue of the partially transposed 4×4 CM V_4. The partial transposition is defined through the following transformation, $\tilde{V}_4 = \mathcal{P}_{1|2}\tilde{V}_4\mathcal{P}_{1|2}$, where $\mathcal{P}_{1|2} = \text{diag}[1,-1,1,1]$, while for a CV tripartite Gaussian state, the quantification is given through the residual contangle, defined as $\mathcal{R}_{i|jk} \equiv C_{i|jk} - C_{i|j} - C_{i|k}$, where $C_{u|v}$ is the contangle of the subsystems u and v (v contains one or two modes). The contangle is a proper entanglement monotone which is defined as the *squared* logarithmic negativity. For calculating this *one-mode-versus-two-modes* logarithmic negativity, one needs to follow the definition of Eq. (8) simply by replacing Ω_2 with $\Omega_3 = \oplus_{j=1}^3 i\sigma_y$ and $\tilde{V}_4$ with $\tilde{V}_6 = \mathcal{P}_{i|jk}V_6\mathcal{P}_{i|jk}$, where the partial transposition matrices are $\mathcal{P}_{1|23} = \text{diag}[1,-1,1,1,1,1]$, $\mathcal{P}_{2|13} = \text{diag}[1,1,1,-1,1,1]$, and $\mathcal{P}_{3|12} = \text{diag}[1,1,1,1,1,-1]$. A *bona fide* quantification of Gaussian tripartite entanglement is given by the minimum residual contangle

$$\mathcal{R}^{\rm min} \equiv \min[\mathcal{R}^{a|mb}, \mathcal{R}^{m|ab}, \mathcal{R}^{b|am}], \tag{9}$$

which guarantees the invariance of tripartite entanglement under all possible permutations of the modes.

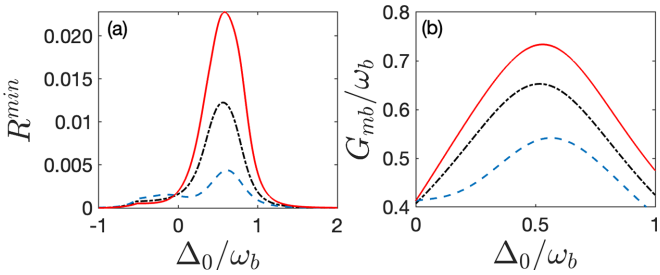

FIG. 2. (a) Magnon-photon-phonon entanglement $\mathcal{R}^{\rm min}$ and (b) effective magnomechanical coupling strength G_{mb}, as a function of the detuning parameter Δ_0/ω_b. The blacked (dashed-dotted), red (solid), and blue (dashed) lines respectively correspond to the nonspinning, CCW-driven, and CW-driven WGM resonator. For the spinning WGM resonator, the Fizeau shift is chosen to be $|\Delta_F/\omega_b| = 0.12$, obtained through $\Omega = 2.4$ kHz.

IV. RESULTS AND DISCUSSION

To start with, in Fig. 2(a) we plot the tripartite entanglement, involving the (driven) cavity, magnon, and phonon modes. For simulation, we use the following set of experimentally feasible parameters [32,63]: $n = 1.44$, $r = 1.1$ mm, $\lambda = 1.5$ μm, $\omega_b/2\pi = 10.627$ MHz, $g_{ma}/2\pi = 5.43$ MHz, $g_{mb}/2\pi = 0.3$ Hz, $\kappa_a/2\pi = 3.87$ MHz, $\kappa_m/2\pi = 1.01$ MHz, $\gamma_b/2\pi = 286$ Hz, $T = 20$ mK, $\omega_d/2\pi = 7$ GHz, and $\epsilon = \sqrt{\frac{2P_{\rm in}\kappa_a}{\hbar\omega_d}}$ (with the driving power $P_{\rm in} = 75$ mW). It is worthwhile to note that the magnon-phonon coupling (g_{mb}) used here is still significantly larger than the experimentally measured one [32], requiring a sphere diameter $D \approx 50$ μm. Instead, one can think of using a low coupling strength by adding a strong drive to the cavity. However, such a strong drive could result in unwanted nonlinear effects, as reported in Ref. [70]. Finally, we set $\Delta_m = \omega_b$, a prerequisite for magnomechanical cooling of the phonon mode. We see that for a nonspinning resonator ($\Omega = 0$), the entanglement is independent of the driving directions, while for the spinning one ($\Omega \neq 0$), it changes by reversing the spinning direction.

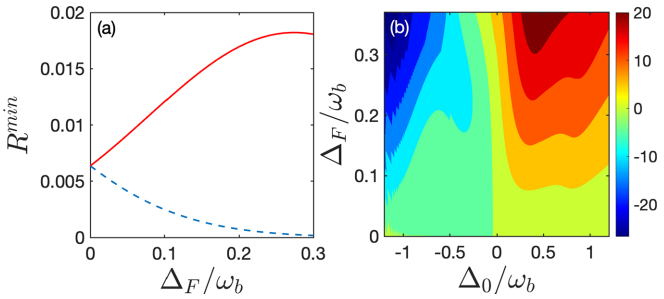

FIG. 3. (a) Magnon-photon-phonon entanglement $\mathcal{R}^{\min}$ vs the Fizeau shift $|\Delta_F/\omega_b|$ at $\Delta_0/\omega_b = 0.5$. The red (solid) and blue (dashed) lines, respectively, represent a spinning CCW- and CW-driven resonator. (b) The isolation factor χ as a function of the detuning Δ_0/ω_b and Fizeau shift $|\Delta_F/\omega_b|$.

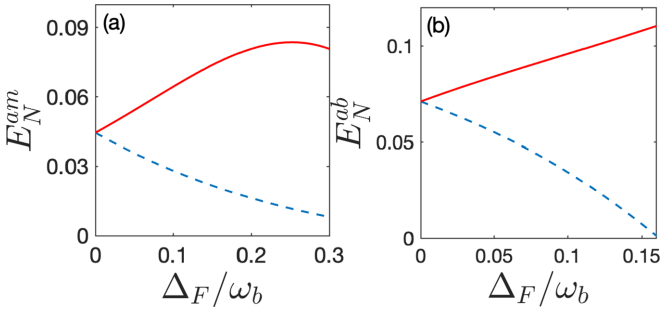

FIG. 4. (a) Cavity-magnon E_N^{am} and (b) cavity-phonon E_N^{ab} entanglement against the Fizeau shift $|\Delta_F/\omega_b|$. The red (solid) and blue (dashed) lines respectively represent the CCW- and CW-driven entanglements. The drive detunings are optimally chosen as $\Delta_0/\omega_b = 0.78$ and $\Delta_0/\omega_b = -0.108$, respectively.

For example, when the maximum entanglement is found for driving the CCW mode, almost no entanglement is observed by driving the CW mode. For a better understanding, in Fig. 2(b) we plot the effective magnon-phonon coupling strength, for varied driving directions. We see that when spinning the resonator, driving the CCW mode enhances the effective magnomechanical coupling strength, while the same gets suppressed by driving the CW mode. Note also that such an observation essentially implies an underlying classical nonreciprocity $\langle m\rangle(\text{CCW}) \neq \langle m\rangle(\text{CW})$. Thus the physics of such nonreciprocal entanglement generation can be understood as follows. In cavity meganomechanics, entanglement occurs due to the magnetostrictive coupling between the magnon-phonon mode, which gets partially transferred to the cavity mode due to the strong magnon-photon interaction. Now, in a spinning resonator different driving induces different coupling amplitudes which along with an optimal detuning condition results in a nonreciprocal formation of quantum entanglement. In passing, we note that for a WGM resonator with a fixed CW spinning direction, one would observe a larger entanglement along the CW direction than the CCW direction.

To further demonstrate the effect of spinning on the nonreciprocal entanglement generation, in Fig. 3(a) we plot the tripartite entanglement at a fixed detuning, against $|\Delta_F/\omega_b|$, for two different driving directions. One can see that while driving the CCW mode significantly enhances the entanglement, driving the CW mode results in enormous suppression. To quantitatively describe the nonreciprocal entanglement, we introduce the isolation factor, defined as

$$\chi = 10\log_{10}\frac{\mathcal{R}^{\min,\circlearrowleft}}{\mathcal{R}^{\min,\circlearrowright}}. \tag{10}$$

Quantum nonreciprocity is said to be achieved for $R^{\min,\circlearrowleft} \neq R^{\min,\circlearrowright}$, i.e., for $\chi \neq 0$. Figure 3(b) depicts the isolation factor χ as a function of the normalized cavity detuning Δ_0/ω_b and the Fizeau shift $|\Delta_F/\omega_b|$. We see that for an optimal choice of parameters, a large isolation of up to 20 dB could be achieved. We note that, to the best of our knowledge, so far such chiral control of quantum entanglement has been reported involving either optical and mechanical modes [22] or optical and microwave modes [60]. Achieving the same for a more complicated three-party system could be an important step forward in realizing chiral quantum networks.

Here, it is also intuitive to examine the other two available forms of entanglements, namely the (driven) cavity-magnon E_N^{am} and the (driven) cavity-phonon entanglement E_N^{ab}. In Fig. 4 we see that both these entanglements also inherit nonreciprocity where driving the resonator from one (CCW) direction significantly enhances the entanglement and driving it from the other (CW) suppresses the entanglement. We also note that the degree of entanglement between the cavity-phonon modes is comparatively higher than the other two. This makes our scheme an alternative route to create strong nonreciprocal photon-phonon entanglement, apart from a cavity optomechanics-based protocol [22].

Finally, we consider an alternative measure for the tripartite quantum entanglement as proposed by Teh and

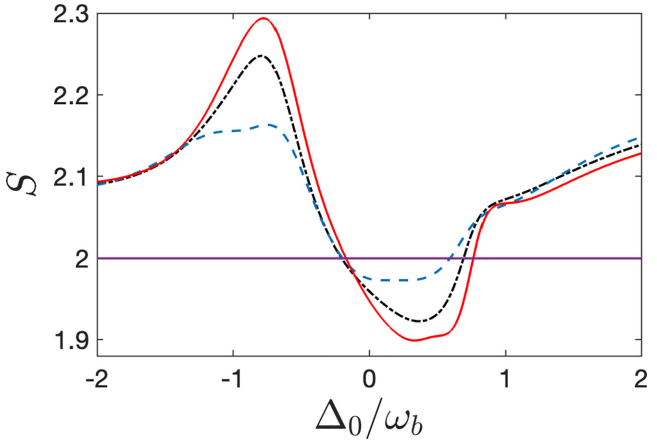

FIG. 5. Tripartite entanglement between the magnon-photon-phonon modes as measured by S with respect to the detuning parameter Δ_0/ω_b. The blacked (dashed-dotted), red (solid), and blue (dashed) lines respectively correspond to the nonspinning, CCW-driven, and CW-driven WGM resonator. The parameters are kept the same as in Fig. 2.

Reid [71]. Here, the emergence of genuine tripartite entanglement is confirmed by the violation of the following inequality (S),

$$\left\langle \left\{ \delta\left[x_{\circlearrowleft,\circlearrowright} - \frac{X+q}{\sqrt{2}} \right] \right\}^2 \right\rangle + \left\langle \left\{ \delta\left[y_{\circlearrowleft,\circlearrowright} + \frac{Y+p}{\sqrt{2}} \right] \right\}^2 \right\rangle \geqslant 2. \tag{11}$$

Notably, a tripartite state is said to be *genuinely* tripartite entangled, if and only if the density operator of the combined three-mode system cannot be represented in a biseparable form. Furthermore, an advantage of using Eq. (11) is it does not require a full estimation of the 8×8 CM, thus it is simpler for experimental implications. Figure 5 shows that the inequality is fulfilled around $\Delta_0 = 0.5\omega_b$ indicating the onset of genuine tripartite entanglement between the cavity-magnon-phonon modes. Driving the resonator from opposite directions respectively results in a stronger and weaker violation of Eq. (11), or in other words, an enhanced and suppressed tripartite magnon-photon-phonon entanglement.

V. CONCLUSION

In conclusion, we have shown how to create nonreciprocal entanglement in a cavity magnomechanical setup. Our scheme relies on the Fizeau light-dragging effect, where spinning the resonator causes a different frequency shift in the counter-propagating modes in a WGM resonator. By placing a YIG sphere inside such a resonator, we are able to show that one can realize nonreciprocal entanglement between the cavity, magnon, and phonon modes. Moreover, with the chosen parameter set, we report an isolation of 20 dB by driving the resonator from opposite sides. Such nonreciprocal formation has also been found in cavity-magnon and cavity-phonon entanglements. Our work opens up possibilities for nonreciprocal quantum control of tripartite entanglement which may find applications in quantum information processing and chiral quantum networking [72,73].

[1] D. L. Sounas and A. Alu, Nat. Photon. **11**, 774 (2017).
[2] L. Fan, J. Wang, L. T. Varghese, H. Shen, B. Niu, Y. Xuan, A. M. Weiner, and M. Qi, Science **335**, 447 (2012).
[3] Q.-T. Cao, H. Wang, C.-H. Dong, H. Jing, R.-S. Liu, X. Chen, L. Ge, Q. Gong, and Y.-F. Xiao, Phys. Rev. Lett. **118**, 033901 (2017).
[4] S. Manipatruni, J. T. Robinson, and M. Lipson, Phys. Rev. Lett. **102**, 213903 (2009).
[5] Z. Shen, Y.-L. Zhang, Y. Chen, C.-L. Zou, Y.-F. Xiao, X.-B. Zou, F.-W. Sun, G.-C. Guo, and C.-H. Dong, Nat. Photon. **10**, 657 (2016).
[6] N. R. Bernier, L. D. Toth, A. Koottandavida, M. A. Ioannou, D. Malz, A. Nunnenkamp, A. K. Feofanov, and T. J. Kippenberg, Nat. Commun. **8**, 604 (2017).
[7] Z. Shen, Y.-L. Zhang, Y. Chen, F.-W. Sun, X.-B. Zou, G.-C. Guo, C.-L. Zou, and C.-H. Dong, Nat. Commun. **9**, 1797 (2018).
[8] N. Bender, S. Factor, J. D. Bodyfelt, H. Ramezani, D. N. Christodoulides, F. M. Ellis, and T. Kottos, Phys. Rev. Lett. **110**, 234101 (2013).
[9] B. Peng, Ş. K. Özdemir, F. Lei, F. Monifi, M. Gianfreda, G. L. Long, S. Fan, F. Nori, C. M. Bender, and L. Yang, Nat. Phys. **10**, 394 (2014).
[10] D.-W. Wang, H.-T. Zhou, M.-J. Guo, J.-X. Zhang, J. Evers, and S.-Y. Zhu, Phys. Rev. Lett. **110**, 093901 (2013).
[11] H. Ramezani, P. K. Jha, Y. Wang, and X. Zhang, Phys. Rev. Lett. **120**, 043901 (2018).
[12] P. Yang, M. Li, X. Han, H. He, G. Li, C.-L. Zou, P. Zhang, Y. Qian, and T. Zhang, Laser Photonics Rev. **17**, 2200574 (2023).
[13] W. Gou, T. Chen, D. Xie, T. Xiao, T.-S. Deng, B. Gadway, W. Yi, and B. Yan, Phys. Rev. Lett. **124**, 070402 (2020).
[14] B. Liang, X. S. Guo, J. Tu, D. Zhang, and J. C. Cheng, Nat. Mater. **9**, 989 (2010).
[15] S. Kim, X. Xu, J. M. Taylor, and G. Bahl, Nat. Commun. **8**, 205 (2017).
[16] R. Fleury, D. L. Sounas, C. F. Sieck, M. R. Haberman, and A. Alù, Science **343**, 516 (2014).
[17] S. Barzanjeh, M. Wulf, M. Peruzzo, M. Kalaee, B. P. Dieterle, O. Painter, and J. M. Fink, Nat. Commun. **8**, 953 (2017).
[18] A. Metelmann and A. A. Clerk, Phys. Rev. X **5**, 021025 (2015).
[19] G. B. Malykin, Phys. Usp. **43**, 1229 (2000).
[20] R. Huang, A. Miranowicz, J.-Q. Liao, F. Nori, and H. Jing, Phys. Rev. Lett. **121**, 153601 (2018).
[21] W. S. Xue, H. Z. Shen, and X. X. Yi, Opt. Lett. **45**, 4424 (2020).
[22] Y.-F. Jiao, S.-D. Zhang, Y.-L. Zhang, A. Miranowicz, L.-M. Kuang, and H. Jing, Phys. Rev. Lett. **125**, 143605 (2020).
[23] B. Z. Rameshti, S. V. Kusminskiy, J. A. Haigh, K. Usami, D. Lachance-Quirion, Y. Nakamura, C.-M. Hu, H. X. Tang, G. E. W. Bauer, and Y. M. Blanter, Phys. Rep. **979**, 1 (2022).
[24] H. Y. Yuan, Y. Cao, A. Kamra, R. A. Duine, and P. Yan, Phys. Rep. **965**, 1 (2022).
[25] X. Zhang, C.-L. Zou, L. Jiang, and H. X. Tang, Phys. Rev. Lett. **113**, 156401 (2014).
[26] Y. Tabuchi, S. Ishino, A. Noguchi, T. Ishikawa, R. Yamazaki, K. Usami, and Y. Nakamura, Science **349**, 405 (2015).
[27] A. Osada, R. Hisatomi, A. Noguchi, Y. Tabuchi, R. Yamazaki, K. Usami, M. Sadgrove, R. Yalla, M. Nomura, and Y. Nakamura, Phys. Rev. Lett. **116**, 223601 (2016).
[28] X. Zhang, N. Zhu, C.-L. Zou, and H. X. Tang, Phys. Rev. Lett. **117**, 123605 (2016).
[29] R. Hisatomi, A. Osada, Y. Tabuchi, T. Ishikawa, A. Noguchi, R. Yamazaki, K. Usami, and Y. Nakamura, Phys. Rev. B **93**, 174427 (2016).
[30] C. Braggio, G. Carugno, M. Guarise, A. Ortolan, and G. Ruoso, Phys. Rev. Lett. **118**, 107205 (2017).
[31] X. Zhang, C.-L. Zou, N. Zhu, F. Marquardt, L. Jiang, and H. X. Tang, Nat. Commun. **6**, 8914 (2015).
[32] X. Zhang, C.-L. Zou, L. Jiang, and H. X. Tang, Sci. Adv. **2**, e1501286 (2016).
[33] K. Ullah, M. T. Naseem, and Ö. E. Müstecaplıoğlu, Phys. Rev. A **102**, 033721 (2020).
[34] X. Li, W.-X. Yang, T. Shui, L. Li, X. Wang, and Z. Wu, J. Appl. Phys. **128**, 233101 (2020).
[35] M.-S. Ding, L. Zheng, and C. Li, Sci. Rep. **9**, 15723 (2019).

[36] C. A. Potts, E. Varga, V. A. S. V. Bittencourt, S. V. Kusminskiy, and J. P. Davis, Phys. Rev. X **11**, 031053 (2021).
[37] M.-S. Ding, L. Zheng, and C. Li, J. Opt. Soc. Am. B **37**, 627 (2020).
[38] B. Sarma, T. Busch, and J. Twamley, New J. Phys. **23**, 043041 (2021).
[39] M. Wang, D. Zhang, X.-H. Li, Y.-Y. Wu, and Z.-Y. Sun, IEEE Photonics J. **11**, 5300108 (2019).
[40] H. Y. Yuan, P. Yan, S. Zheng, Q. Y. He, K. Xia, and M.-H. Yung, Phys. Rev. Lett. **124**, 053602 (2020).
[41] M. Aspelmeyer, T. J. Kippenberg, and F. Marquardt, Rev. Mod. Phys. **86**, 1391 (2014).
[42] A. K. Sarma, S. Chakraborty, and S. Kalita, AVS Quantum Sci. **3**, 015901 (2021).
[43] R. Riedinger, A. Wallucks, I. Marinković, C. Löschnauer, M. Aspelmeyer, S. Hong, and S. Gröblacher, Nature (London) **556**, 473 (2018).
[44] C. F. Ockeloen-Korppi, E. Damskägg, J.-M. Pirkkalainen, M. Asjad, A. A. Clerk, F. Massel, M. J. Woolley, and M. A. Sillanpää, Nature (London) **556**, 478 (2018).
[45] S. Barzanjeh, E. S. Redchenko, M. Peruzzo, M. Wulf, D. P. Lewis, G. Arnold, and J. M. Fink, Nature (London) **570**, 480 (2019).
[46] J. Li, S.-Y. Zhu, and G. S. Agarwal, Phys. Rev. Lett. **121**, 203601 (2018).
[47] J. Li, S.-Y. Zhu, and G. S. Agarwal, Phys. Rev. A **99**, 021801(R) (2019).
[48] Z. Zhang, M. O. Scully, and G. S. Agarwal, Phys. Rev. Res. **1**, 023021 (2019).
[49] J. Li and S.-Y. Zhu, New J. Phys. **21**, 085001 (2019).
[50] H. Y. Yuan, S. Zheng, Z. Ficek, Q. Y. He, and M.-H. Yung, Phys. Rev. B **101**, 014419 (2020).
[51] M. Yu, S.-Y. Zhu, and J. Li, J. Phys. B: At., Mol. Opt. Phys. **53**, 065402 (2020).
[52] J. M. P. Nair and G. S. Agarwal, Appl. Phys. Lett. **117**, 084001 (2020).
[53] M. Yu, H. Shen, and J. Li, Phys. Rev. Lett. **124**, 213604 (2020).
[54] J. Li and S. Gröblacher, Quantum Sci. Technol. **6**, 024005 (2021).
[55] Y.-P. Wang, J. W. Rao, Y. Yang, P.-C. Xu, Y. S. Gui, B. M. Yao, J. Q. You, and C.-M. Hu, Phys. Rev. Lett. **123**, 127202 (2019).
[56] N. Zhu, X. Han, C.-L. Zou, M. Xu, and H. X. Tang, Phys. Rev. A **101**, 043842 (2020).
[57] Y.-j. Xu and J. Song, Opt. Lett. **46**, 5276 (2021).
[58] Y. Xu, J.-Y. Liu, W. Liu, and Y.-F. Xiao, Phys. Rev. A **103**, 053501 (2021).
[59] Z.-B. Yang, J.-S. Liu, A.-D. Zhu, H.-Y. Liu, and R.-C. Yang, Ann. Phys. **532**, 2000196 (2020).
[60] Y.-l. Ren, Opt. Lett. **47**, 1125 (2022).
[61] M. M. Cunha, A. Fonseca, and E. O. Silva, Universe **5**, 209 (2019).
[62] A. Francis, J. K. Freericks, and A. F. Kemper, Phys. Rev. B **101**, 014411 (2020).
[63] S. Maayani, R. Dahan, Y. Kligerman, E. Moses, A. U. Hassan, H. Jing, F. Nori, D. N. Christodoulides, and T. Carmon, Nature (London) **558**, 569 (2018).
[64] C. W. Gardiner and P. Zoller, *Quantum Noise: A Handbook of Markovian and Non-Markovian Quantum Stochastic Methods with Applications to Quantum Optics* (Springer, Berlin, 2000).
[65] D. Vitali, S. Gigan, A. Ferreira, H. R. Böhm, P. Tombesi, A. Guerreiro, V. Vedral, A. Zeilinger, and M. Aspelmeyer, Phys. Rev. Lett. **98**, 030405 (2007).
[66] G. Vidal and R. F. Werner, Phys. Rev. A **65**, 032314 (2002).
[67] M. B. Plenio, Phys. Rev. Lett. **95**, 090503 (2005).
[68] G. Adesso and F. Illuminati, J. Phys. A: Math. Theor. **40**, 7821 (2007).
[69] V. Coffman, J. Kundu, and W. K. Wootters, Phys. Rev. A **61**, 052306 (2000).
[70] M. Ludwig, B. Kubala, and F. Marquardt, New J. Phys. **10**, 095013 (2008).
[71] R. Y. Teh and M. D. Reid, Phys. Rev. A **90**, 062337 (2014).
[72] H. Yonezawa, T. Aoki, and A. Furusawa, Nature (London) **431**, 430 (2004).
[73] Z. Kurucz, P. Adam, Z. Kis, and J. Janszky, Phys. Rev. A **72**, 052315 (2005).